



ORR Reactivity of Surface Ni Along with Pt Surface in Pt-Ni Surface

Venkataramana Imandi, Prafulla Puri and Abhijit Chatterjee

EasyChair preprints are intended for rapid dissemination of research results and are integrated with the rest of EasyChair.

December 20, 2020

ORR reactivity of surface Ni along with Pt surface in Pt-Ni surface

Venkataramana Imandi¹, Prafulla Puri¹ and Abhijit Chatterjee²

1. Wainganga college of engineering and management, Nagpur, India
2. Department of Chemical Engineering, Indian Institute of Technology Bombay, Mumbai, India

Abstract: Nanoporous Pt-Ni more specific are synthesized via selective dissolution of Ni attains a more catalytic activity towards oxygen reduction reaction (ORR). With the help of kinetic Monte Carlo simulation, we observed that change in the nanoporous Pt-Ni is separate from the very known Pt high in the first layer of Platinum-Nickel catalytic surface. In the Platinum-Nickel, first layer and second layer both are high in Pt. A less quantity of Ni is stays on the first layer. With help of density functional theory, ORR speeds up several orders because of surface Ni atoms. We considered various Platinum-Nickel configurations in this paper. production of OH is the rate-determining step based on our reports in the ORR. At lower amount of Ni, nanoporous Pt-Ni shows 8 times more ORR than pure Pt catalyst.

Keywords: ORR, density functional theory, nanoporous

1. Introduction:

The oxygen reduction reaction (ORR) is very importance to lower-temperature fuel cell applications¹. The highest ORR activity is described in the literature with a skin layer of Pt(111) on an elongated Platinum-Nickel alloy surface, that possesses an reactivity about 80 orders more than that of unmixed Platinum(without even small Ni atoms present on the surface) catalyst². The existence of a low-cost, more availability in the nature, Pt-Ni catalyst more active than pure and used for gaining the structure information of the oxygen reduction reaction at the Pt and Pt-Ni first layer^{3,4}. Herein, we are keen in the Platinum-Nickel evolution and dissolution. Snyder et al. observed that nonmaterial can provide ORR activity of Pt-Ni is more active than that of Pt. It has been given that while going form Platinum-Nickel(111) first layer to Platinum-skin (top surface is completely Platinum) ORR activity loss from 5 fold to 3 fold and subsurface is Ni rich or Pt rich could be approximately about 10 order high reactive than first layer Pt surface. It shows reactivity of Pt-Ni nanoporous and including a Pt skin are not similar to each other⁵. The main region of the high Pt-Ni ORR activity is comparatively less studied than Pt-first layer. The main aim of this work is to report Pt-skin using DFT studies.

Very high reactivity in the Pt-skin than pure Pt is originated from density functional theory (DFT) studies. Herein, the first layer has Pt, and the layer below first layer is 90% Nickel or in some other categories 60-90% Ni⁶. At close to equilibrium, Platinum is known to preferentially comes to the upper layer in Pt₃Ni alloys. Because of computational vibrations, Platinum-Nickel surface is to assumed that there is no Nickel in the below surface layer. To clarify more understanding; assumption has 90% Ni is stayed at further below with respect to surface layer. On the basis of this assumption, Pt/Ni distribution, DFT reports have targeted on nanoparticles^{5,7} and first layer of Platinum(111), (100), and (110) models⁸. Based on the calculated activation barriers on Pt-Ni surface and unreconstructed Platinum(100) surface, H₂O formation is the rate-activation step on both Platinum(100) and Platinum/Nickel(100) surface, OH production

is the rate-determining step on the Platinum(111) and oxygen molecule decomposition is the rate-determining step on Platinum(111) surface⁹. Due to Strain, subsurface and whole Nickel play a critical form on the binding of adsorbents' on the Platinum-Nickel surface. A review of Platinum-Nickel alloys activity of catalyst at operating conditions of fuel cell is provided in ref¹⁰.

Pt–Ni catalyst is not similar from nanoporous Pt-Ni. Pt–Ni nanoporous is prepared from close to dissolution of Ni from Pt–Ni metal. Ni is soluble from the alloy from top layer to subsurface layer, a Pt-rich nanoporous material is finally formed that shows less quantity of Ni at the top layer. The second layer and further below layers are rich in Pt. As the dissolution process continues, less coordinated sites, Ni is present at those under coordinated sites along with existence of terrace sites for larger time. With the help of DFT, it is assumed that presence of Ni on the first layer in high content Pt first layer increase the catalytic activity. The importance of surface Ni in the porous Pt and Pt-Ni slab models, ORR is absent. To obtain the region of more reactivity of Pt-Ni, we used (i) distribution of elements within the Pt-Ni catalyst and (ii) distribution effects on the ORR understanding.

First, changing of Pt-Ni structure is analyzed with respect to time using the kinetic Monte Carlo (KMC) method. Kinetic Monte Carlo information is great element to study the diffusion and reaction involving dissolution within experimentally more time scales. An 18 nanometer Platinum-Nickel nanoparticle was studied at higher potential and high temperature. Our resultant structure obtains large number of steps and edges on {111}-oriented facets. Our relevant finding is that less quantity of Ni is in the first layer. We reported a more number of DFT results based on various Platinum-Nickel elemental confirmations obtained from KMC simulations. The density functional theory calculations results obtained that the existence of Ni in the first layer increase the ORR reactivity on Platinum-Nickel catalyst than pure Pt catalytic surface.

The conference paper is separated into the the order section. Information of the DFT methods are discussed in section 2. The obtained reports are analyzed into section 3. Conclusions are analyzed in section4.

2. Methods:

2.1 Density Function Theory Calculations. DFT framework within ab initio calculations were analyzed with the Vienna Ab Initio Simulation Package software package¹¹. The ultra soft pseudopotentials for H, O, Ni, and Pt are used¹². Our ORR consists of three primary steps as explained later. Through DFT calculations, Rate-determining step is obtained and the effect of first layer Ni is also obtained. On the basis of assumption that OH can attach greatly to the less coordination sites, e.g., at steps, due to this more surface sites not accessible for further reaction. So, we used slab calculations. The Pt-Ni(111) surface calculations are done using a 3×2 surface with estimated lattice constant is 3.99 Å. The 3.92 Å is the experimental lattice constant of Pt. The surface consists 4 layers within every layer, 12 are kept as Pt atoms. The computational box dimension was 8.443 Å \times 9.749 Å \times 9.192 Å. Along z-direction, vacuum space of 10 Å were kept to remove spurious interaction among consequent images. For exchange-correlation functional generalized gradient functional was used, in which the PW91 functional¹³ was used. The kinetic energy cutoff for planewave was of 350 eV which is to be enough for our simulations. Methfessel-Paxton of smearing parameter 0.2 eV along with order 1 can be used. The last bottom surface was fixed to their experimental lattice constant conformations, on the other hand upper three layers were agreed to freed from their positions. Using quasi-Newton algorithm was used for ionic optimization. The force tolerance of 0.001 eV/Å was used throughout the simulations. For self-consistent calculations, Davidson algorithm was used, and its limit were 10^{-5} . A $2 \times 2 \times 1$ k-point sampling for the Brillouin zone and which includes Gamma point was used for all the computational. The lowest activation path was analyzed with the help of nudged elastic band method using seven images. The largest energy image in that path was analyzed to be near to the saddle location. A spring

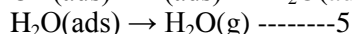
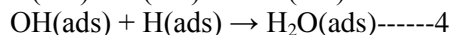
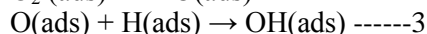
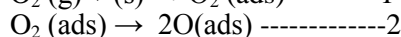
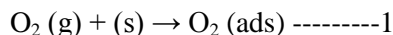
constant of $5.0 \text{ eV/\text{Å}^2}$ can be utilized to remove images from moving to their position.

To influence the influence of water on the oxygen reduction reaction process, we used approach in the reference of¹⁴. Surface Pt was studied utilizing a $3 \times 2 \times 1$ slab, each layer has 12 atoms. On the above of surface Pt, an one layer of aqueous solution i.e, $2 \times 2 \times 1$ dimension is created. The water layer consists of 8 water molecules. Alternative water molecules (OH part) are aligned towards metal first layer(H-down). The remaining OH bonds are parallel to the metal surface. On the Pt and Pt-Ni surface, oxygen molecule was kept by removing 2 water molecules. One water molecule is removed for OH and H_2O formation reaction on the metal surfaces. To limit our computational resources, zero or one Ni atoms in Pt surfaces were considered.

Previous experiments^{15,16} and theoretical¹⁷ results reports shows Pt(100) first layer attains to hexagonal phase due to binding of oxygen molecule. We have done calculations on the {111}-surfaces, which area is more than {100}-surface. ORR rates contingent on the first layer Pt-Ni atoms configurations. The influence of surface Ni atoms can speed up the reaction or not studied extensively by keeping one, two, three and four Ni atoms kept on the Pt-first layer. The ensemble of atoms should effects a catalytic properties atom at the first layer which modify physical component of the ensemble is modified is called as the ensemble effect.

3. RESULTS:

3.1. Binding Energies of elementary Species. The oxygen reduction reaction mechanism consists of the following reaction steps:



We started by calculating the more stable binding adsorption sites for oxygen atom(ads), hydrogen atom(ads), hydroxyl(ads), and water(ads). On the stable sites, main reaction will occur. To influence of Nickel on the surface, we kept one or two Nickel elements on the Pt-first layer and estimate the absorption energies for over the atom, connection between atoms, and three fold sites conformations (fcc and hcp). Few of binding sites are shown in Figure 1. Atoms of 2 Ni present on the surface, the relevant picture is shown by Figure 1b. The notation was assumed that the three fold atom sites are represented by three metal atoms on which adsorbents adsorbed. For example, a Platinum–Platinum–Platinum hcp site indicates that 3 Platinum and 0Nickel form the site. Similarly a Platinum-Nickel-Nickel hcp site indicates that there is participation of One Platinum and two Nickel atoms. The fcc site for 3Pt is far away from the Pt+1Ni surface site. Same labeling are utilized for the top and bridge sites. Total of 20 absorption energy simulations were studied for O(adsorbate), H(adsorbate), OH(adsorbate), and H_2O (adsorbate) to include of major arrangements. Adsorption energies were estimated as difference from adsorbate on the surface to only adsorbate energy in the vacuum and whole surface without adsorbate energy.

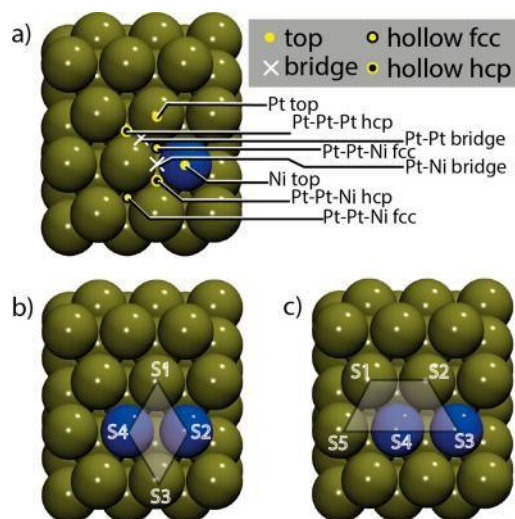


Figure 1. (a) Many absorption sites on Platinum–Nickel surface. Configuration of Platinum–Nickel atoms was assumed; (b) O₂ dissociation for S1–S4 and (c) OH production and water formation on S1– S5 represented by the shown polygon. Other than blue Ni atoms are Pt.

3.1.1. H Binding. The fcc site is strongest absorption binding site for H (Figure 2). Binding energies on fcc(face centered cubic) is -0.30 eV, hexagonal close packed (hcp) is -0.25eV, bridge site is -0.24eV, and top sites is -0.18eV in pure Pt surface. For Platinum+1Nickel and Platinum+2Nickel, H strongly binds in the close proximity of Ni, than in the close proximity of Pt surface layer. For instance, for 2Platinum+Nickel, fcc site is strongest adsorption energy a adsorption energy of -0.38 eV that is more favorable than face centered cubic(3Pt) site (-0.33 eV) in Platinum+1Nickel. In same manner, fcc sites on 2Platinum-Nickel and Platinum-2Nickel with adsorption energies are -0.37 and -0.44 eV, accordingly.

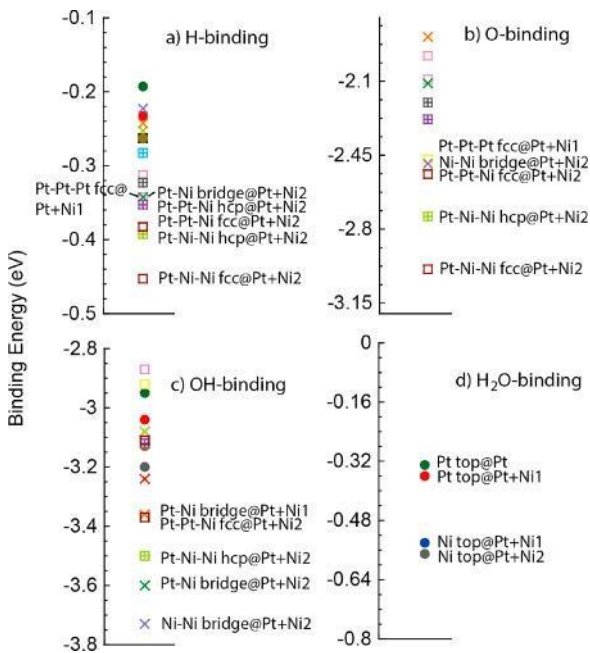


Figure 2. Largest binding energy sites for chemisorbed (a) Hydrogen, (b) Oxygen, (c) hydroxyl, and (d) water.

3.1.2. O Binding. According to dissociation of O₂, on Pt and Pt-Ni surface, two atomic oxygen are formed. Fcc site is the atomic oxygen strongly binds on Pt(111) surface. hcp, bridge and top positions are the following binding sites for O binding with a adsorption energy of -1.98 eV. O₂ absorbs highly in the neighboring places of Ni than that on pure Pt (observe Figure 2b). For example, a binding energy of bridge site on 2Platinum-Nickel and Platinum-2Nickel fcc sites are -2.47 and -2.99 eV. The fcc site of 3Pt in Platinum+1Nickel is found to be more adsorption energy of -2.09 eV, that was more than compared to unmixed Platinum. It shows that binding energy increases to close proximity of Ni and decreases way away from the Nickel surface site. Same phenomena are found for hcp, bridge and top configurations.

3.1.3. OH Binding. Bridge site is the strongest site for Pt-first layer with an adsorption energy of -3.08 eV. Top site with an adsorption energy of -2.95 eV is found, on the other hand, weakest binding site is observed at hcp site (-2.20 eV). Unstable fcc site for OH is observed on pure Pt surface. However, stable binding sites for Pt+1Ni and Pt_2Ni were observed. Compared to pure Pt, Platinum-Nickel bridge site is for 1Ni + Pt and for Pt+2Ni, bridge site for Nickel-Platinum/Nickel–Nickel is the strongest binding energy. Ni-top and Pt-top positions are least binding energies. These top sites are followed by

hexagonal close packing (hcp) and face centric cubic sites.

3.1.4. H₂O Binding. On first layer Pt, Pt top is highest binding energy for H₂O with a adsorption energy of -0.33 eV. Other than top sites, there are no stable sites for H₂O adsorption. Ni-top position site is the strongest at Pt-Ni1 configuration with an adsorption energy of -0.54 eV which was more than the top position of Pt top with an adsorption energy of -0.36 eV. Top position of Ni on Platinum+2Nickel is the strongest adsorption energy of -0.57 eV.

In the final report, O and H strongly favors fcc sites, chemisorbed OH adsorbs tightly at the bridge coformation, and water binds at top position sites. All configurations, the surface Nickel favors binding sites and obtains stronger binding energies.

3.2. Activated energy barriers of elementary reactions. Activated energy barriers for reactions 2-4 are discussed in the next text.

3.2.1. O₂ Decomposition. An O₂ molecule stays at the top-fcc site of first layer of Pt(111) and first layer of Platinum-Nickel(111) with orient in the planar to the metal first layer with tilted away. This conformation is called the molecular precursor state (MPS) (see diagram 3). The bond lengths of oxygen-oxygen on the

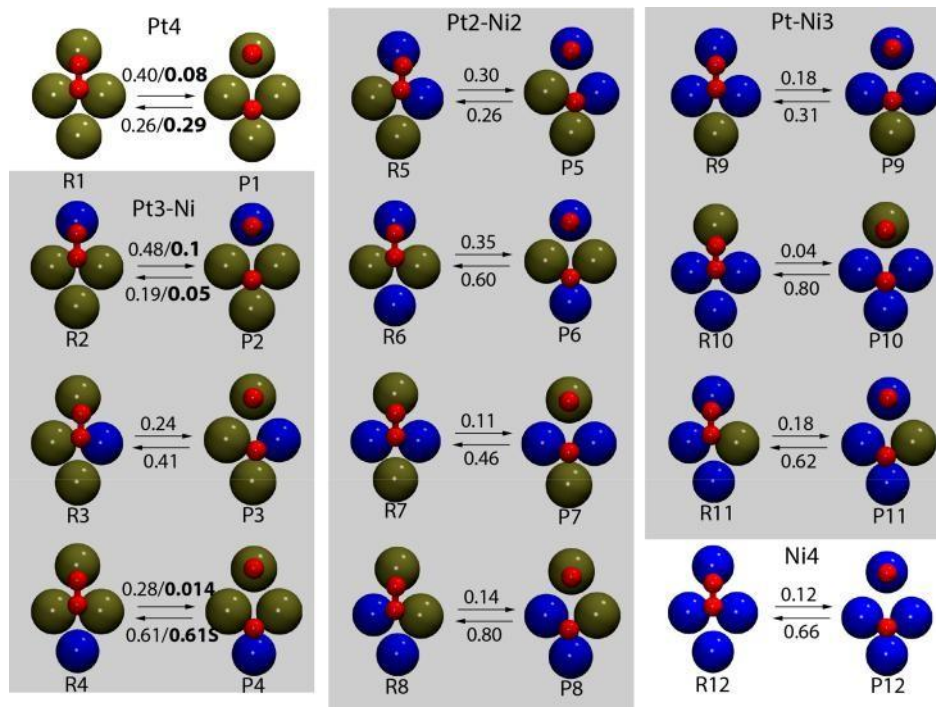


Figure 3. Molecular precursor state(initial state) and final state of O₂(ads) decomposition on pure Platinum and Platinum-Nickel(111) surfaces: green are (Pt), blue are (Ni), and red are (oxygen). Activated barriers are in eV, for onward and backward reactions are shown on the arrows. S1-S4 metal atoms of Figure 1b are shown. Barriers are shown in boldface in the of aqueous solution.

Pt(111) surface in the initial configuration, saddle point, and final configuration 1.47, 2.16, and 3.39 Å, respectively. Top-hcp sites were considered for all O-O bonding confirmations on pure Platinum and Platinum-Nickel first layer (see Figure 3).

On pure Pt, the onward and backward barriers with respect to initial state are 0.40 eV and 0.26 eV. The energy barriers for pure Platinum and Platinum-Nickel first layer are calculated based on the with influence of Ni atoms on the absorption energy of of initial state and product O elements. Adsorption energies for the absorbed two oxygen elements at those configurations estimated utilizing from subtracting surface energy with binding oxygen molecule to surface energy without oxygen molecule and oxygen molecule in the vacuum. The 2 various atomic oxygen absorption energy at a far of 3.39 Å on

Platinum(111) was -2.13 eV. The adsorption energies of -2.4 , -2.81 , and -2.63 belong to P1, P2, and P3 product configurations are, respectively, with separate oxygen atoms distance was found to be P1(3.20), P2(3.22), and P3(3.64) Å, respectively. Stronger adsorption energy of oxygen atom at the hexagonal close packed (hcp) absorption to Nickel (P3) obtains in the less activated kinetic barrier for O_2 decomposition (see diagram 3). Using surface two Ni atoms for configurations for P6, P7, and P8, same phenomena is found.

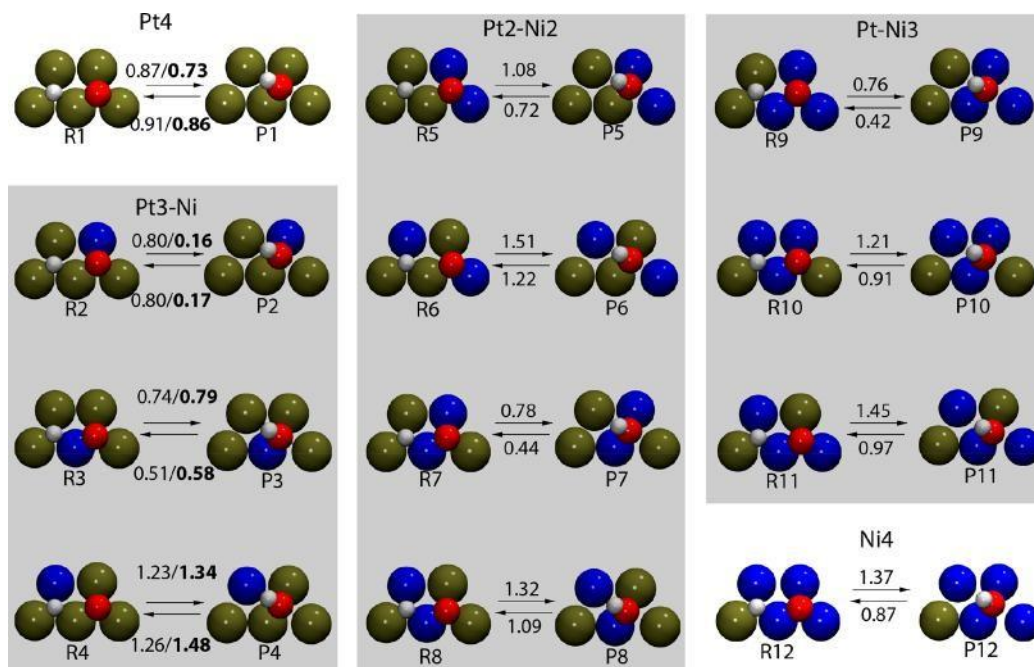


Figure 4. Initial configuration (chemisorbed O with chemisorbed H) and final configuration (OH adsorbed) on pure Platinum and Platinum–Nickel surface: green are shown (Pt), blue are (Ni), red are (O), and white are (H). Above and below arrow values are forward and reverse barriers. S1–S5 atoms of Figure 1c are shown. On water, the barriers are in the fold face.

Based on the results, we observed that the replacement of Platinum with Nickel on (111) first layer (Platinum–Nickel alloys) reveals increase ORR reactivity for O_2 decomposition. Presence of oxygen at the hcp site, it is due to Nickel present in the hcp site. At 300K, the arrangement R3-P3 is more kinetic rate than the arrangement R1-P1 by assuming same frequency factors for the above said final states. Increase in the reaction kinetic rates was observed for two Ni atoms and more than two Ni atoms in first layer of Pt surface than pure Pt surface.

3.2.2. OH production. For O and H adsorption states, the most favorable sites of these adsorbents' are fcc positions, i.e., were assumed of the initial confirmation of equation 3. For OH, bridge site is more stable. Nickel at the S5 position, this results in increase in highest activated energy. To decrease the number of arrangements, we did not keep at S5 position, rather kept at the S1-S4 position in Figure 1c. S5 position is kept as Pt, which reduces the binding energy of H first layer in the initial configuration is lower. Figure 4 reveals the more stable initial and final configuration for the genesis reaction of OH.

On pure Pt first layer, the forward and reverse activated energies for OH productin are 0.87 and 0.91 eV, respectively. For R2-P2 and R3-P3 arrangements, onward and backward activated energies are decreased by substitution of Pt by Nickel. Based on the estimated onward and backward activated energies for the Platinum–one-Nickel arrangements in diagram 4, it reveals for few configurations, the production of OH is endergonic. Substitution of two Platinum with Nickel atoms, the calculated onward and backward reaction energies are higher than first layer Pt surface. For Pt-Ni3 and N4 arrangements, same conclusions are made. The more stable initial state, saddle point, and final

configuration of different configurations are shown in the figure 4.

3.2.3. H₂O production. H₂O production, our report kept OH at the bridge position and H is kept at the fcc position. Top sites are only the binding energies for H₂O binding, we kept H₂O at the top position on the Platinum and Platinum-Nickel surface in figure 5.

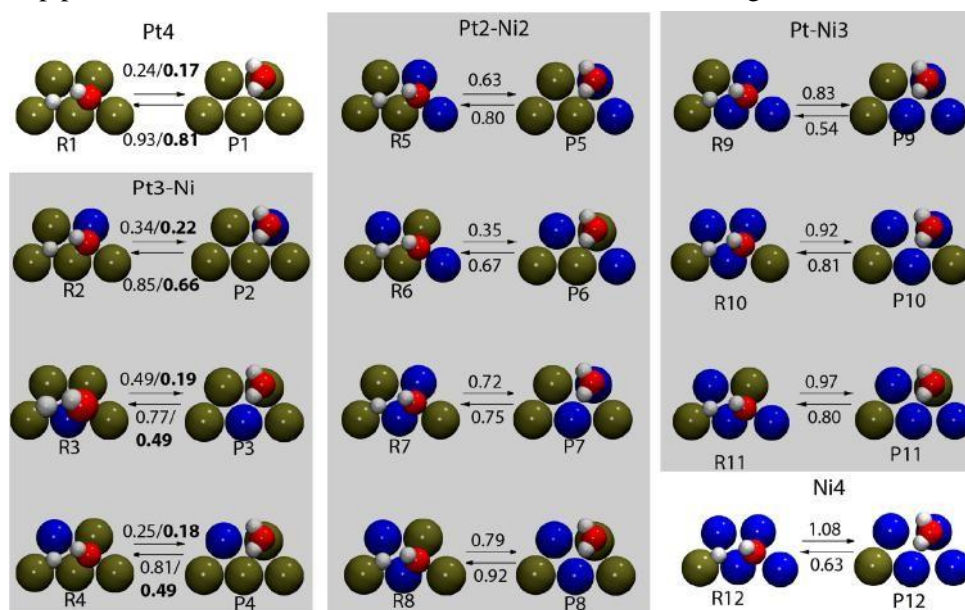


Figure 5. Initial configuration(chemisorbed OH and chemisorbed H) and final configuration(chemisorbed H₂O) on first layer Platinum and Platinum-Nickel arrangements are appeared. Atom colors: green are by (Pt), blue are by (Ni), red are (oxygen), and white are (hydrogen). Values above and below arrows are forward and reverse barriers. Other than atoms of above figure are shown in Figure 1c. On water, barriers are shown in boldface.

Figure 5 gives optimized reactant, product on pure Pt and Pt-Ni various configurations. Onward and backward activated energies are 0.24 and 0.93 eV on the pure Platinum-surface. By substituting Pt with Ni, there is increase in the binding energy as well as the reaction barriers and exothermicity will decrease. The reactions have more endothermic when surface has 3 or more Ni atoms. This is due to strongest absorption sites on the Ni present on the surface. In conclusion, not absence of Ni cannot speed up the formation reaction of H₂O. Accordingly, not absence of Nickel at the S5 position, OH production leads to increase in the adsorption energy which results increase in the activation barrier. Therefore, we did not kept Nickel at the S5 configuration in diagram 5.

In conclusion, the activated energies calculated in the figure 3-5, we observe that rate activated step is OH production on the Platinum first layer and Pt-Ni arrangements first layer. By substituting one Ni on the Pt surface, which can increase OH formation nearly 100 time than the pure Pt catalyst at 300K.

We calculated the equilibrium constant for all the rearrangements. We assumed equal frequency factors for forward and reverse reactions. Equilibrium constant K_{eq} is determined from calculating both forward and backward rates and $K_{equilibrium} = k_{onward}/k_{backward}$, where k_{onward} and $k_{backward}$ relates the onward and backward rate constants. Higher equilibrium constant says that greater driving force for forward reaction and hence reaction is exothermic. Pt-Ni surface configurations, obtained ratio of forward and backward constant are greater than 1 for one and two Ni surface atoms and less than one for 3 and four Ni atoms on the metal surface. For three and four Ni surface atoms, the reverse reaction is more favorable. Relevant pathways are obtained from all kinetic pathways. On the basis of onward and back barriers and ratio of forward and backward, surface with pure Pt and surface with one Ni on the surface have more kinetic rates and to study of the ORR.

In the experiments, the Platinum–Nickel catalytic surface is used in the confirmation of water solvent. To unravel the influence of water, we have done more calculations using explicit water on the pure Pt surface and Platinum+one-Nickel and Platinum+two-Nickel first layer. The bold numbers represent activation barriers in Figures 3–5. OH formation is again would be activated step on Platinum first layer and in the confirmation of water. Regarding the activated OH production arrangement (eq 3), R2-P2 gives a rate constant and low activated energy barriers. Those arrangements mainly give OH production. The activated energy for the step R2-P2 and R1-P1 in Figure 4 is 0.16eV and 0.73eV on Pt-Ni catalytic surface and Pt catalysts. In other way, the equilibrium constant would be lesser than one and large activation barriers observed for other configurations. Those steps do not give important quantities of genesis of OH and decomposition of OH and not observed thermodynamically relative to the oxygen reduction reaction.

For OH formation, the R2-P2 step can be increased in the 10 times quantity over the R1-P1 arrangement. The ratio of Ni:Pt is as lowest as 1:400, it is observed that, rate-determining arrangement three times quantity faster than on Platinum-Nickel first layer that of pure Pt catalyst surface. Equilibrium constant greater than one is obtained for R2-P2 configuration.

Recently, enhanced experiments showed that oxygen reduction reactivity in nonmaterial Platinum-Nickel by order of 48 times more than over commercial Platinum/Carbon catalytic surface. Our KMC simulations reveal that a more amount of under coordinated sites on the metal first layer is existed. However, such sites strongly bound species like OH, there will be problem for further reactions. Moreover, the small concentration of Ni on the surface cannot induce stress and show large ORR activity. Nonetheless, the large access of Ni on the surface can lead to decrease in the oxygen reduction reaction activity.

Finally, using DFT and pseudo potentials, this has been observed that Pt comes to first layer from subsurface layer. The results provide Pt segregation can occur with two approaches. The results shows that a less quantity of first layer Nickel (0.0004–0.012) at close to with 97% Pt. Moreover, the nonporous Platinum-Nickel is studied at away from reactive conditions. Activated thermodynamic computation shows that less number of Ni is present on the surface of Pt.

Conclusions:

Two conclusive aspects were observed, precisely, (i) the atom probability of of Pt-Ni in Platinum/Nickel in porous materials Pt–Ni and (ii) oxygen reduction reaction reactivity due to the small concentration of Nickel on the metal surface. Our KMC simulations proved that a less concentration of Nickel stays on the Pt metallic first layer. The fraction f Ni on the Pt-surface is less than 10^{-3} . Additionally, Pt is rich in the subsurface layer. DFT calculations are performed on the Pt and Pt-Ni surface and shows that Pt₃Ni atom arrangement can be more catalytic than pure Pt first layer. The OH-production is the activated-determining step for both the first layer Pt and less quantity of Nickel on the first layer Pt atoms. Due to fewer fractions of surface Ni atoms on the Pt metal first layer, the rate of formation on first layer Nickel would be 8 quantity of magnitude more than pure Pt first layer. Low fraction of Ni cannot be seen through experimental techniques such as like electron diffraction and photoelectron spectroscopy X-ray. More information of higher activity of Pt-skin in nonporous catalytic surface is required.

AUTHOR INFORMATION

Corresponding Author

*E-mail: abhijit@che.iitb.ac.in.

ORCID

Abhijit Chatterjee: 0000-0002-3747-8433

Notes

The authors declare no competing financial interest.

References:

- ¹ M. Shao, Q. Chang, J.-P. Dodelet, and R. Chenitz, *Chem. Rev.* **116**, 3594 (2016).
- ² V.R. Stamenkovic, B. Fowler, B.S. Mun, G. Wang, P.N. Ross, C.A. Lucas, and N.M. Markovic, *Science* (80-.). **315**, 493 (2007).
- ³ L. Sementa, O. Andreussi, W.A. Goddard, and A. Fortunelli, *Catal. Sci. Technol.* **6**, 6901 (2016).
- ⁴ P. Feibelman, S. Esch, and T. Michely, *Phys. Rev. Lett.* **77**, 2257 (1996).
- ⁵ C. Cui, L. Gan, H.H. Li, S.H. Yu, M. Heggen, and P. Strasser, *Nano Lett.* **12**, 5885 (2012).
- ⁶ I. Matanović, F.H. Garzon, and N.J. Henson, *J. Phys. Chem. C* **115**, 10640 (2011).
- ⁷ V.R. Stamenkovic, B.S. Mun, M. Arenz, K.J.J. Mayrhofer, C. a Lucas, G.F. Wang, P.N. Ross, and N.M. Markovic, *Nat. Mater.* **6**, 241 (2007).
- ⁸ S.-W. Chou, Y.-R. Lai, Y.Y. Yang, C.-Y. Tang, M. Hayashi, H.-C. Chen, H.-L. Chen, and P.-T. Chou, *J. Catal.* **309**, 343 (2014).
- ⁹ Z. Duan and G. Wang, *J. Phys. Chem. C* **117**, 6284 (2013).
- ¹⁰ Y. Bing, H. Liu, L. Zhang, D. Ghosh, and J. Zhang, *Chem. Soc. Rev.* **39**, 2184 (2010).
- ¹¹ G. Kresse and J. Furthmüller, *Phys. Rev. B* **54**, 11169 (1996).
- ¹² D. Vanderbilt, *Phys. Rev. B* **41**, 7892 (1990).
- ¹³ J. Perdew, J. Chevary, S. Vosko, K. Jackson, M. Pederson, D. Singh, and C. Fiolhais, *Phys. Rev. B* **46**, 6671 (1992).
- ¹⁴ H. Chen, *Curr. Protein Pept. Sci.* **7**, 101 (2006).
- ¹⁵ A. Borg, A.M. Hilmen, and E. Bergene, *Surf. Sci.* **306**, 10 (1994).
- ¹⁶ M.A. Van Hove, R.J. Koestner, P.C. Stair, J.P. Bibérian, L.L. Kesmodel, I. Bartoš, and G.A. Somorjai, *Surf. Sci.* **103**, 218 (1981).
- ¹⁷ P. Havu, V. Blum, V. Havu, P. Rinke, and M. Scheffler, *Phys. Rev. B* **82**, 161418 (2010).